H1 preliminary

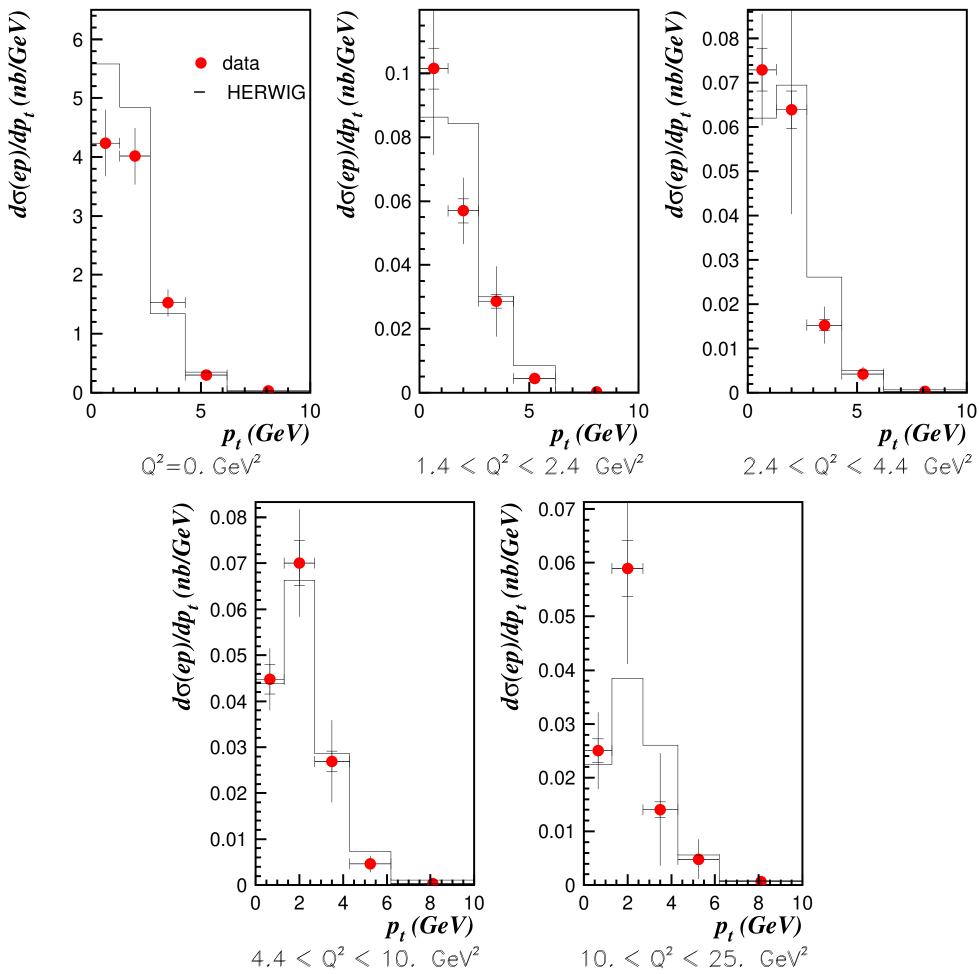

Figure 1: The differential cross section $d\sigma/dp_t$ of the photon remnant jet for data (circles) and HERWIG model (histogram) in the intervals of the virtuality Q^2 corresponding to the resolved component for $x_\gamma < 0.75$, $p_T^{(i)} > 5$ GeV, $p_T^{(1)} + p_T^{(2)} > 12.$ GeV and $-3. < \eta^{(i)} < 0.$ ($p_T^{(i)}$ and $\eta^{(i)}$ are the transverse momenta and the pseudorapidities of the two jets with the highest transverse momentum in γ^*p system). The distribution of the intrinsic momentum k_t of the parton coming to the hard process in HERWIG was taken as Gaussian $dN/\mathrm{dp}_\mathrm{T}^2 \propto \exp(-\mathrm{k}_\mathrm{T}^2/\mathrm{k}_0^2)$ with the default value $k_0 = 0.66$ GeV.

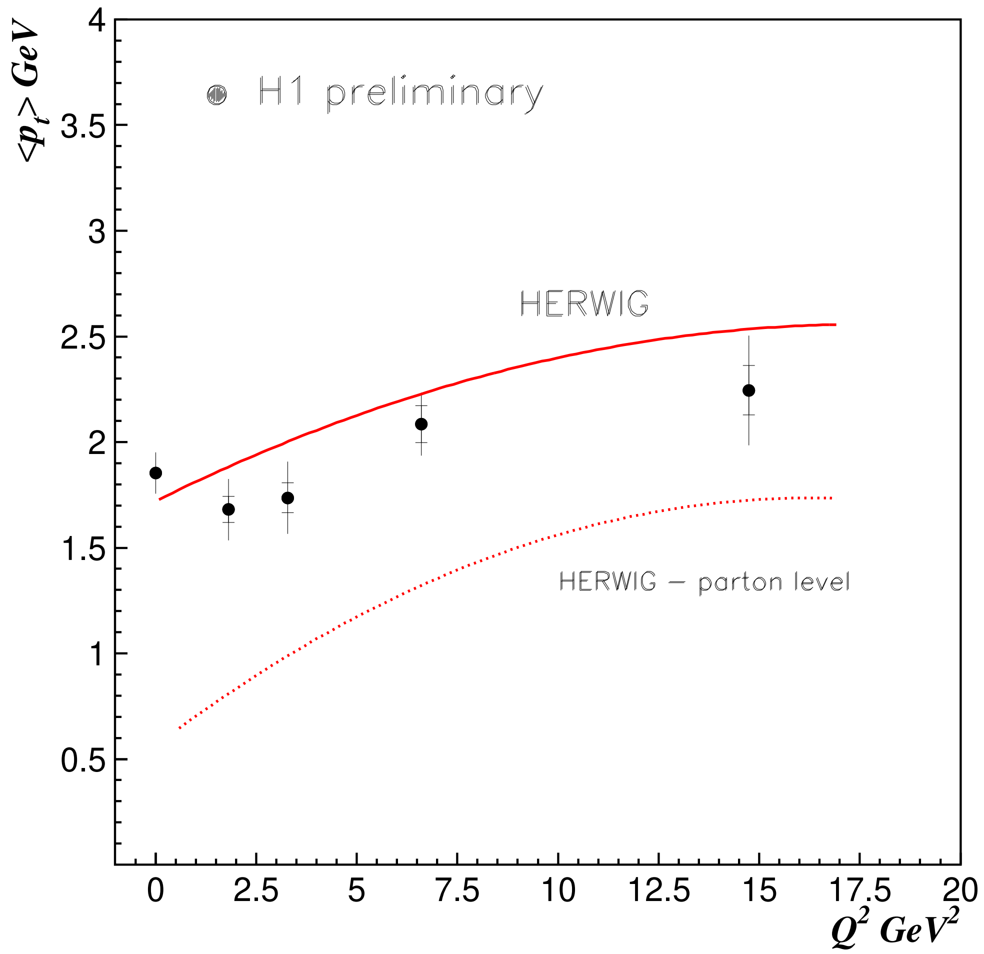

Figure 2: The mean value of the photon remnant jet p_t for data (circles) and HERWIG model (curve) in dependence on the virtuality Q^2 corresponding to the resolved component for $x_\gamma < 0.75$, $p_T^{(i)} > 5$ GeV, $p_T^{(1)} + p_T^{(2)} > 12.$ GeV and $-3. < \eta^{(i)} < 0.$ ($p_T^{(i)}$ and $\eta^{(i)}$ are the transverse momenta and the pseudorapidities of the two jets with the highest transverse momentum in γ^*p system). The distribution of the intrinsic momentum k_t of the parton coming to the hard process in HERWIG was taken as Gaussian $dN/\mathrm{dp_T^2} \propto \exp(-\mathrm{k_T^2/k_0^2})$ with the default value $k_0 = 0.66$ GeV.

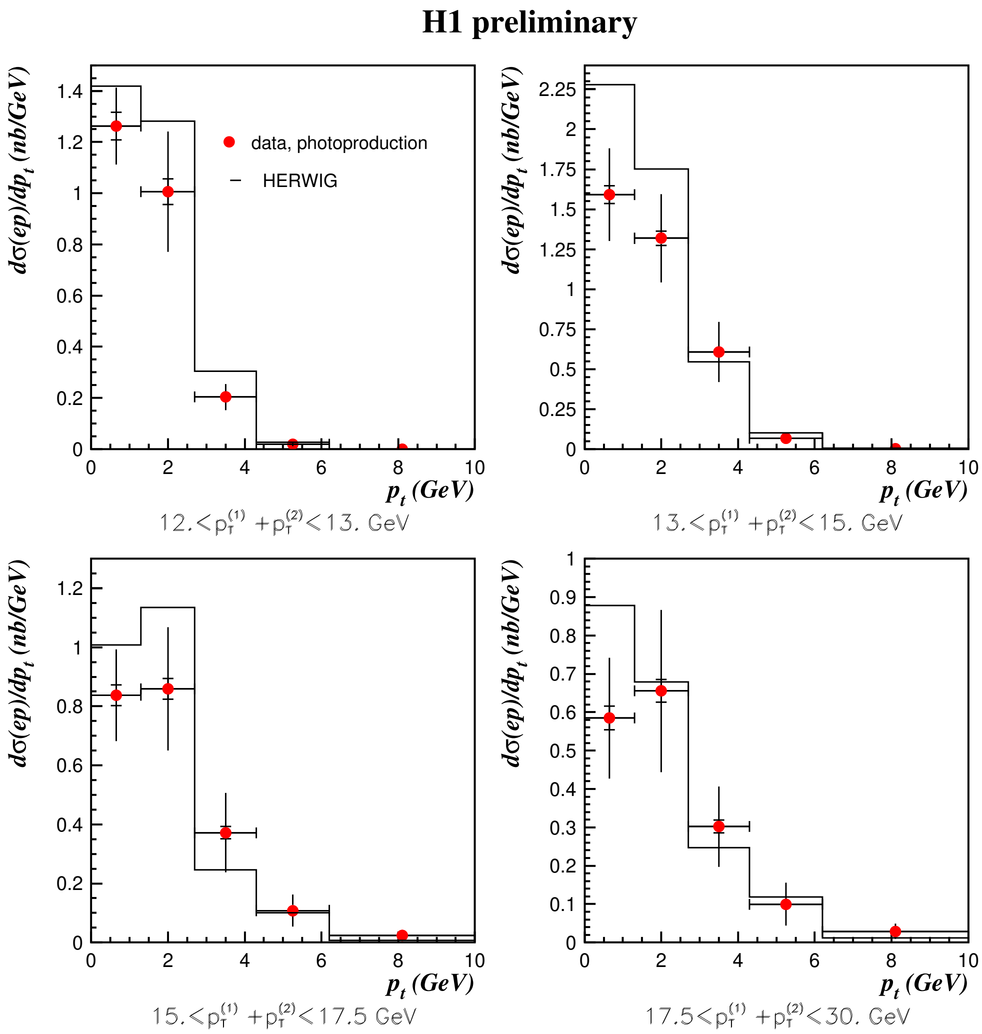

Figure 3: The differential cross section $d\sigma/dp_t$ of the photon remnant jet for the photoproduction data (circles) and HERWIG model (histogram) in four intervals of the hard scale $p_T^{(1)} + p_T^{(2)}$ corresponding to the resolved component for $x_\gamma < 0.75$, $p_T^{(i)} > 5$ GeV and $-3. < \eta^{(i)} < 0.$ ($p_T^{(i)}$ and $\eta^{(i)}$ are the transverse momentum and the pseudorapidities of the two jets with the highest transverse momentum in γ^*p system). The distribution of the intrinsic momentum k_t of the parton coming to the hard process in HERWIG was taken as Gaussian $dN/\mathrm{dp_T^2} \propto \exp(-\mathrm{k_T^2/k_0^2})$ with the default value $k_0 = 0.66$ GeV.

H1 preliminary

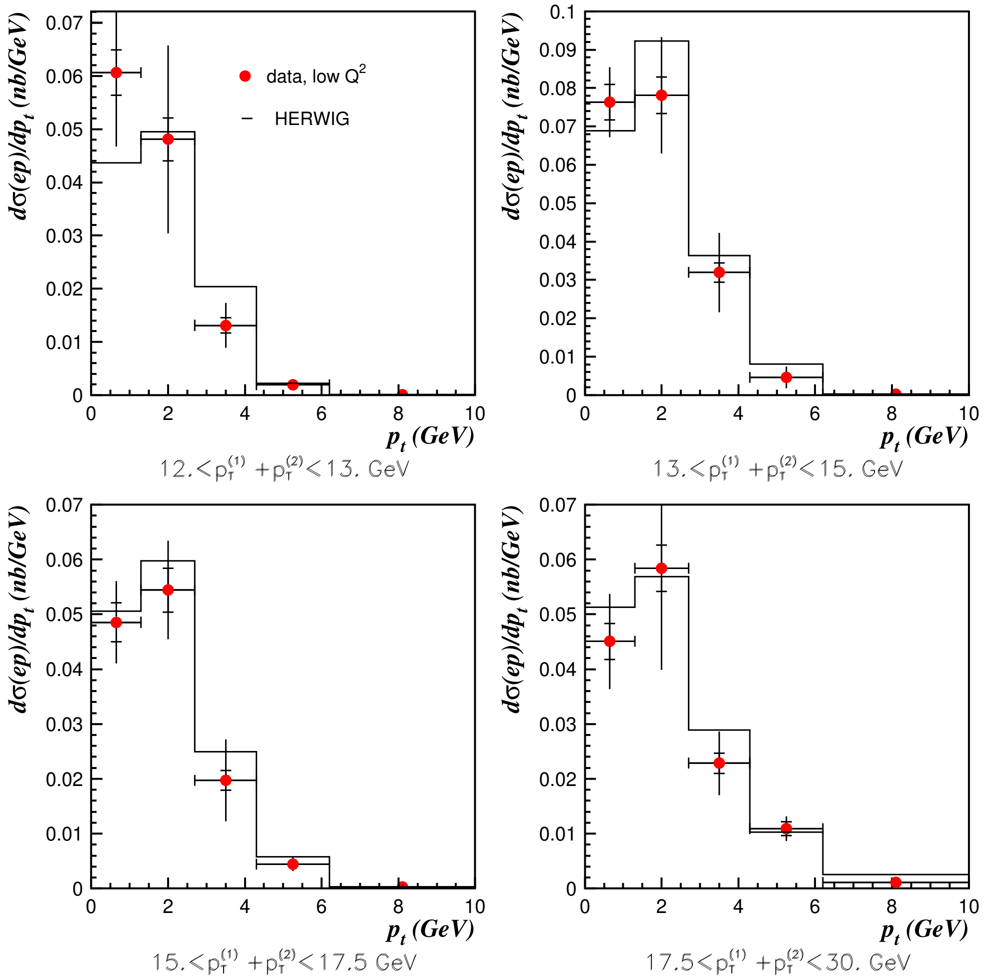

Figure 4: The differential cross section $d\sigma/dp_t$ of the photon remnant jet for low Q^2 data (circles) and HERWIG model (histogram) in four intervals of the hard scale $p_T^{(1)} + p_T^{(2)}$ corresponding to the resolved component for $x_\gamma < 0.75$, $p_T^{(i)} > 5$ GeV and $-3. < \eta^{(i)} < 0.$ ($p_T^{(i)}$ and $\eta^{(i)}$ are the transverse momenta and the pseudorapidities of the two jets with the highest transverse momentum in γ^*p system). The distribution of the intrinsic momentum k_t of the parton coming to the hard process in HERWIG was taken as Gaussian $dN/\mathrm{dp}_\mathrm{T}^2 \propto \exp(-\mathrm{k}_\mathrm{T}^2/\mathrm{k}_0^2)$ with the default value $k_0 = 0.66$ GeV.

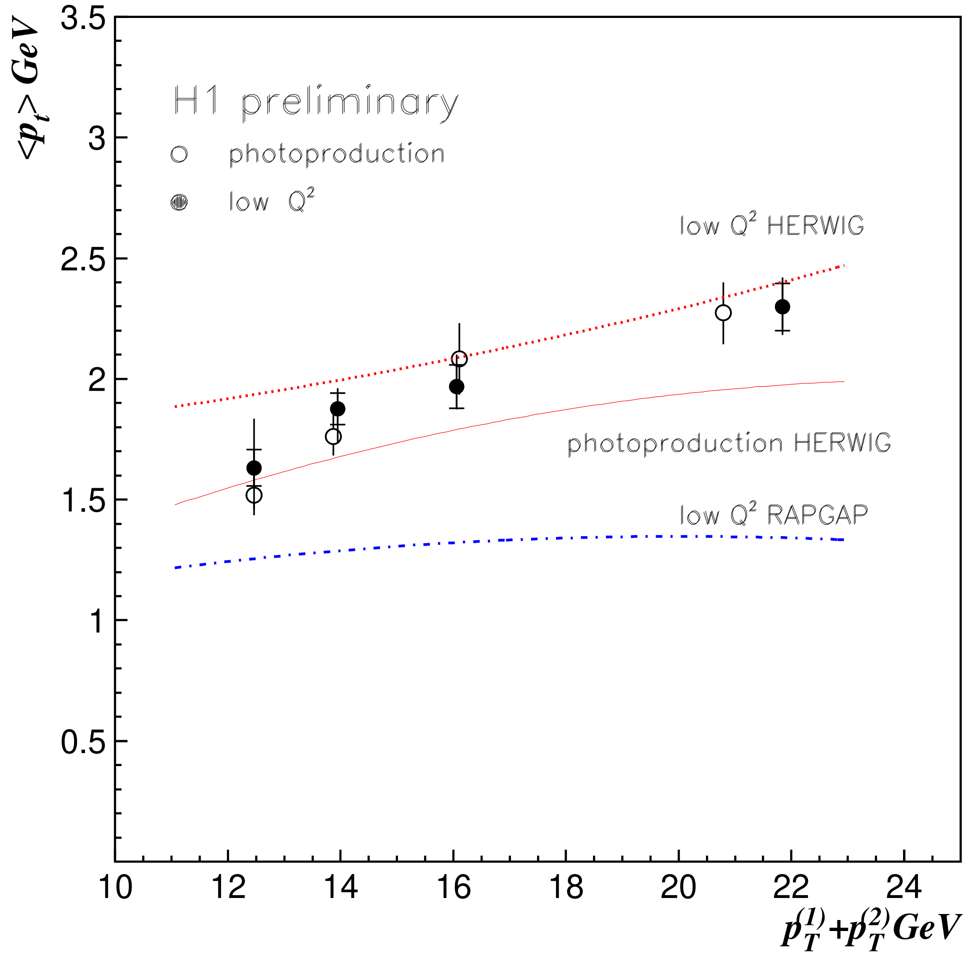

Figure 5: The mean value of the photon remnant jet p_t for the photoproduction (open circles) and low Q^2 (full circles) data as a function of the hard scale $p_T^{(1)} + p_T^{(2)}$ corresponding to the resolved component for $x_\gamma < 0.75$, $p_T^{(i)} > 5$ GeV and $-3 < \eta^{(i)} < 0$ ($p_T^{(i)}$ and $\eta^{(i)}$ are the transverse momenta and the pseudorapidities of the two jets with the highest transverse momentum in γ^*p system), compared with the HERWIG and RAPGAP MC predictions. The distribution of the intrinsic momentum k_t of the parton coming to the hard process in HERWIG and RAPGAP was taken as Gaussian $dN/\mathrm{dp}_\mathrm{T}^2 \propto \exp(-\mathrm{k}_\mathrm{T}^2/\mathrm{k}_0^2)$ with the value $k_0 = 0.66$ GeV.